Nearby Young Solar Analogs: I. Catalog and Stellar Characteristics

Eric J. Gaidos
Jet Propulsion Laboratory
California Institute of Technology
Mail Stop 170-25
Pasadena, CA 91125
gaidos@gps.caltech.edu

ABSTRACT

We present a catalog of 38 young solar analogs within 25 pc, stars which are uniquely well-suited for observations of their circumstellar environments to improve our understanding of conditions within the Solar System during the Hadean/early Archean eons (prior to 3.8 Ga). These G and early K stars were selected from the *Hipparcos* astrometric catalog based on lack of known stellar companions within 800 AU, bolometric luminosities close to that of the zero-age Sun and consistent with the zero-age main sequence, and *ROSAT* X-ray luminosities commensurate with the higher rotation rate and level of dynamo-driven activity in solar-mass stars less than 0.8 Gy old. While many of these objects have been previously identified, this sample is novel in two respects: The selection criteria specifically consider the planetary environment, and the selection is uniform and all-sky. The X-ray emission from these young analogs is spectrally soft and consistent with a coronal origin. Calcium H and K emission, rotation periods, lithium abundances, and kinematics support an age range of 0.2 to 0.8 Gy for most of these stars. Three stars have exceptionally high space motions with respect to the Local Standard of Rest and may be old disk or halo stars which are anomalously X-ray luminous.

Subject headings: solar neighborhood, stars: activity, stars: late-type, stars: planetary systems

origin of life
early Earth
astrobiology

1. Background

The first several hundred My of the Earth's history were of great significance to our origins: The Hadean and early Archean eons saw the appearence of liquid water on the surface, a period of unknown prebiotic chemistry, and probably the emergence of recognizable biological organisms. Similar conditions may have prevailed on the surfaces of Mars until a divergence towards its radically different present state. However, nearly all terrestrial record of that early epoch has

been lost in the recycling of the Earth's crust by plate tectonics and the gradual alteration of crustal, atmospheric, and oceanic chemistry over geologic time. The oldest known terrestrial minerals (Australian zircons) date to at most 4.2 Ga (Maas *et al.* 1992), the oldest known rocks, Wopmay gneisses, to 3.96 Ga (Bowring *et al.* 1989), and the oldest known geological units in Archean shields only to 3.8 Ga. Rare gas isotopic abundances provide only crude constraints on the composition of the primitive atmosphere (Kasting 1993) and the better-preserved surfaces of Mars and the Moon offer only indirect and poorly chronometered information.

External conditions in the Solar System could have profoundly influenced the early surface environments of Earth and other terrestrial planets. These are (1) the luminosity evolution of the Sun; (2) a stronger solar wind; (3) a higher ultraviolet flux; and (4) a higher cratering rate. Standard stellar theory predicts a solar luminosity 70-75% of the present value prior to 3.8 Ga, requiring elevated levels of atmospheric greenhouse gases to maintain temperatures above the freezing point of water (Kasting 1991). Alternatively, a solar mass loss of order 5% (through the solar wind) would have attenuated this luminosity evolution (Boothroyd *et al.* 1991; Graedel *et al.* 1991; Whitmire *et al.* 1995). The more rapidly rotating and chromospherically active young Sun produced a stronger solar wind and higher ultraviolet emission (Feigelson 1982; Sonett *et al.* 1991). A strong solar wind could have eroded the primitive atmospheres of the terrestrial plnaets, especially those lacking the protection of magnetic fields (Perez-de-Tejada 1992; Jakosky *et al.* 1994; Chassefiere 1997). In the absence of an oxygen-derived ozone shield, ultraviolet radiation would have reached the Earth's lower atmosphere and surface, driving photochemistry and creating a distinct, if not difficult environment for biota (Zahnle & Walker 1982; Canuto *et al.* 1982; Canuto *et al.* 1983). The Earth also experienced a period of intense bombardment prior to 3.8 Ga (Weissman 1989, Chyba 1991). This "Late Heavy Bombardment", possibly associated with the clearing of residual planetesimals in the outer Solar System (Fernandez & Ip 1983), may have produced biotic precursor molecules by shock heating (Fegley *et al.* 1986) and contributed significant amounts of volatiles and organics (Chyba 1987; Ip & Fernandez 1988; Chyba *et al.* 1990). On the other hand, very large impacts would have vaporized the entire ocean or even the upper crust, extinguishing an existing biosphere (Maher & Stevenson 1988).

The study of young stars closely resembling the early Sun is one strategy in understanding the circumsolar environment of the early Earth. The ongoing formation of stars like the Sun provides a "time machine" by which we can directly observe conditions that may have existed in our own Solar System. A large number of such young solar analogs must be studied to explore the potential diversity of cirumstellar environments. This approach also compensates for the limited observational criteria for establishing analogies and our primitive understanding of planet formation and evolution: Our own planetary system, containing a planet which supports a biosphere and a sentient species, is not necessarily typical (Wetherill 1994).

Studies of early Solar System analogs have primarily focused on stars with clear evidence for circumstellar gas or dust (e.g., Aumann *et al.* 1984; Smith & Terrile 1984; Walker & Wolstencroft 1988; Aumann & Probst 1991; Stencel & Backman 1991; Cheng *et al.* 1992; Backman & Paresce

1993; Sargent & Beckwith 1994; Kalas & Jewitt 1996; Waelens *et al.* 1996; Beckwith & Sargent 1996; McCaughrean & O'Dell 1996; Fajardo-Acosta *et al.* 1997; Mannings & Sargent 1997; Chen *et al.* 1998). This material may be the early stages or debris of planetary systems. However, many of these objects (such as pre-main sequence and T Tauri stars) only represent the first $\sim$ 10 My of Solar System history, and the analogy of others (such as the A stars) with the early Solar System is poorly established. There has been relatively little work on unbiased samples of young main sequence stars (Tsikoudi 1989; Tsikoudi 1990; Gahm *et al.* 1994; Jewitt 1994; Ray *et al.* 1995; Moneti *et al.* 1997). Observations of stars selected *a priori* as young solar analogs are needed for a more complete picture of possible Solar System conditions during the Hadean and early Archean eons.

Young solar-mass stars can be identified by their high rotation rate (e.g., Fekel 1997), chromospheric activity (e.g., Henry *et al.* 1996), spottedness (e.g., Lockwood *et al.* 1997), and coronal X-ray emission (e.g., Sterzik & Schmitt 1997) relative to their older counterparts. Other techniques include lithium abundance (e.g., Favata *et al.* 1997), space motions (Eggen 1995), and the existence of a more massive companion of known age (Lindroos 1986). A few analogs have been studied in great astrophysical detail (Dorren & Guinan 1994; Dorren *et al.* 1995; Landi *et al.* 1997; Güdel *et al.* 1997a; Güdel *et al.* 1997b; Strassmeier & Rice, 1998). The release of all-sky surveys by the *Hipparcos* astrometric and *ROSAT* X-ray space observatories has now made the construction of a complete, uniform, and well-defined sample selected on zero-age main sequence status and high levels of coronal X-ray emission feasible.

Here, a set of quantitative optical and X-ray criteria are developed to identify analogs to the Sun prior to 3.8 Ga. A catalog of nearby young solar analogs is constructed by applying these criteria to *Hipparcos* stars within 25 pc. Astrophysical properties of these stars published in the refereed literature are presented and analyzed. While many of the individual objects have been previously identified as young solar-mass stars, this sample is novel in two respects: The selection criteria are specifically designed from the point of view of the planetary environment, and the selection is uniform and all-sky. It is presented here as a catalog of practical size ideal for future observational programs. The criteria for selecting these stars is developed in §2 and the construction of the catalog is presented in §3. §4 contains a brief analysis of the nature of the X-ray emission from these stars. Finally, §5 presents age-related properties indicating stellar youth.

2. Selection Criteria

Young solar analogs are selected from stars within 25 pc using criteria developed to describe the Sun and its environment more than 3.8 Ga. Stars within 25 pc are relatively easy to study and this distance is similar to the completeness limits of the input catalogs (see 3).

2.1. Duplicity

Since the Sun is by all appearances a single star – notwithstanding speculation on the existence of a "Nemesis" companion (Davis *et al.* 1984) – and stellar companions can have profound consequences for the dynamical evolution of planetary systems (Holman *et al.* 1997), strict analogy would dictate the exclusion of all stars with companions. Clearly, stars with companions at separations on the scale of the Solar System should be excluded. However, there are sound reasons to retain some wide binary systems for study: First, many visual binary systems have not been confirmed as physical systems (by observations of common proper motion) and may actually be spurious optical pairs. Second, the properties of a very high-mass or very low mass coeval companion may constrain the age of the system (e.g., Lindroos 1986).

The final reason is more hypothetical: Wide binaries (those with semi-major axes $a \sim 10^4$ AU) are weakly bound systems: The tidal field of the Galactic disk, plus the perturbing effects of passing stars and molecular clouds, may disrupt an appreciable fraction of these systems over the main sequence lifetime of solar mass stars. Membership in wide binary systems may be more frequent among, even representative of, young stars. It is even conceivable that the Sun was once in a binary system which became unbound sometime in the past. Approximate lower limits to the initial semi-major axis of a hypothetical Sun-companion system can be inferred from two facts: The orbits of the outer planets have not been disrupted, and the system was not so tightly bound that it would have survived for 4.6 Gy. (A companion would result in significant disruption of the Oort comet cloud at $a \sim 10^4$ AU However, the time required for the tidal field of the Galaxy to isotropize the cloud is only 5×10^8 yr (Heisler & Tremaine 1986) and thus evidence of any such disturbances would have been subsequently erased.)

The dynamical effects of a stellar companion depend on the tidal field felt by the planetary system, the inclination of the companion's orbit relative to the ecliptic plane, and the time scale of the orbital period relative to the periods of the planetary secular resonances. The orbital planes of binaries systems with separations larger than 30-40 AU are not preferentially aligned with the stellar spin axes (Hale 1994) and thus large inclinations are likely. "Short-period" companions alter planetary orbits independent of each other, while "long-period" companions cause the entire system only to precess as a unit. Innanen *et al.* (1997) have performed billion-year integrations of the orbits of the outer giant planets and found them to be stable against the perturbative effects of a 0.05 $M_\odot$ companion on a 400 AU circular orbit, for all inclination angles. This result, scaled by preserving the tidal field M/a^3, indicates that similar stability would occur for a 1 $M_\odot$ companion on a $\sim$ 1000 AU orbit. Weinberg *et al.* (1987), using Monte Carlo calculations, estimated that over 90% of binaries with $a < 2000$ AU would survive for 4.6 Gy. This result is weakly dependent on certain assumptions about the mass and size of molecular clouds.

In conclusion, binary systems with semi-major axes less than 1000 AU are very unlikely to resemble the early Solar System. While these objects may be interesting in their own right, they are poor analogs and will not be considered here. Since the orbital period corresponding to

$a = 1000$ AU is 3×10^4 years no orbital elements will be available for these systems. Instead, the semimajor axis must be statistically estimated from the projected spatial separation at the single epoch of observation: The median value of the ratio of semimajor axis to projected separation for an ensemble of orbits with an isotropic projection distribution and the canonical eccentricity distribution $f(e) = 2e$ is 1.26. Thus stars with companions within a projected linear distance of 800 AU are excluded from the sample. The corresponding angular separation limit is 32 arc-seconds at the 25 pc limit of the sample, a fortuitous correspondence with the resolution limit of the *ROSAT* X-ray observations used to select stars (§3).

2.2. Bolometric Luminosity, Temperature & Metallicity

The physics and chemistry at a distance a from a star of luminosity L will depend in large part on the characteristic temperature of a blackbody in equilibrium with insolation, a quantity which is proportional to $L^{1/4}a^{-1/2}$. The run of temperature with semi-major axis will determine the minimum distances where silicates and ices are stable against sublimation and may profoundly shape the formation and subsequent evolution of any planetary system (Stevenson & Lunine 1988). The dynamical time scales within a hypothetical planetary system which has been cleared of nebular gas scale with orbital period, which is proportional to $a^{3/2}M^{-1/2}$. The author proposes that the best analogy is attained when the equilibrium temperature as a function of orbital period is the same around another star. This scaling requires that the quantity $LM^{-2/3}$ be invariant.

The mass of the Sun is assumed to have remained constant over its history, although this will not prevent the sample being used to test the hypothesis of significant mass loss. The zero-age Sun was a G4/5 star with $L \approx 0.69L_\odot$ and $M = 1M_\odot$ (barring significant mass loss) and stars are selected using an "analogy parameter"

$$A = (L/0.69)M^{-2/3}, \tag{1}$$

where L and M are in solar units. "Good" solar analogs are required to have analogy parameters within the range $2/3 < A < 3/2$, a criterion which essentially selects G stars. While the mass of single stars cannot be accurately measured, a theoretical zero-age main sequence (ZAMS) can be used to relate mass to the observable luminosities and effective photospheric temperatures. Thus a range of acceptable A values can be mapped to ranges of acceptable luminosities and effective temperatures.

Stellar metallicity is important in defining solar analogs: It determines the position of the ZAMS in the Hertzsprung-Russel diagram, affects the amount of spectral line blanketing and stellar ultraviolet emission, and may be an important indicator of the mean abundance of heavy elements in the progenitor protostellar nebula and the presence of solid bodies around a star (Gonzalez 1997). Spectroscopic measurements of metallicities are not available for most stars and are not directly used as a selection criterion here (Abundances obtained *post facto* for selected stars will be reported). However, a solar metallicity ZAMS is used to calculate limits on luminosity

and effective temperature: The requirement $2/3 < A < 3/2$ corresponds to a mass range of $0.89 < M/M_{\odot} < 1.09$ and a luminosity range $-0.37 < \log_{10} L/L_{\odot} < 0.04$ (Perryman *et al.* 1998). The luminosity evolution of the constant-mass Sun has been empirically described by Gough (1981);

$$L/L_{\odot} = [1 + 0.4\,(1 - t/t_0)]^{-1}\,, \tag{2}$$

where t/t_0 is the ratio of the age to the present age of 4.6 Gy. The expected luminosity change over the 0.8 Gy age range of the sample is 5%. The bright end of the luminosity range is relaxed accordingly, leading to a final criterion of $-0.37 < \log_{10} L/L_{\odot} < 0.06$. This corresponds approximately to spectral types G0 through K1.

Within this luminosity range, stars are selected based on their location near the solar-metallicity ZAMS in the H-R diagram. A limit is placed on the allowed distance from the solar ZAMS to preferentially eliminate evolved stars and unresolved multiple systems. Of course, single stars with non-solar metallicities will also deviate from the solar ZAMS and the cut-off must be reasonable to avoid eliminating too many objects. Here, the main sequence of the Hyades cluster is used as the cut-off, forming the upper boundary of the selection region in the H-R diagram (Fig. 1). The Hyades main sequence has been constructed and its age (625 ± 50 Ma) established using *Hipparcos* astrometric data (Perryman *et al.* 1998). It is metal-rich ([Fe/H] = +0.14) compared to other open clusters and field stars (Boesgaard 1989; Carraro & Chiosi 1994; Cayrel de Strobel *et al.* 1997). Because of the cluster's relatively high metallicity and age near the 0.8 Gy selection limit, its stars will be among the most luminous (at a given effective temperature) of acceptable young G stars, making the Hyades ZAMS an ideal luminosity limit. It happens that no lower luminosity (low metallicity) criterion is necessary as no under-luminous candidates are identified.

2.3. Activity

The early luminosity evolution of solar-mass stars is slow (~1% per 150 Ma) and initially parallel to the zero-age main sequence. Without independent mass and metallicity information it is not possible to estimate the ages of field stars based on position in the H-R diagram alone. Fortunately, a more dramatic evolution in rotation rate and associated dynamo-driven activity occurs: The loss of angular momentum through a magnetized wind drives a secular decrease in rotation rate, chromospheric activity, and coronal X-ray luminosity thoughout the main sequence lifetimes of solar-mass stars. The correlations between age, rotation rate, activity, and soft (< 1 keV) coronal X-ray emission have been well established by observations of other solar-mass stars (Schmitt *et al.* 1985; Maggio *et al.* 1990; Walter & Barry 1991; Mathioudakis *et al.* 1995; Schmitt *et al.* 1995; Fleming *et al.* 1995; Baliunas *et al.* 1996; Hempelmann *et al.* 1996).

Coronal X-ray emission is an appropriate stellar chronometer for G dwarf stars much older than ~ 70 My (the age of the Pleiades cluster), ages at which the initial star-to-star dispersion in rotation rates and X-ray emission has been diminished by the stronger winds and faster

deceleration of the more rapid rotators (Stauffer & Soderblom 1991). While the age of any particular G star cannot be accurately derived from its X-ray emission, a *sample* of young solar-mass stars can be constructed in a statistically sound manner. [By contrast, stars earlier than late F have weak or nonexistent coronae (Schmitt *et al.* 1985; Simon *et al.* 1995; Simon & Landsman 1997; Wolff & Simon 1997) while stars later than early K exhibit large and variable X-ray luminosities (Fleming *et al.* 1995; Giampapa *et al.* 1996; Drake *et al.* 1996).] X-ray emission also does not suffer from projection effects, is only weakly absorbed by the interstellar medium and can be detected across a volume of space sufficiently large to find an interesting number of candidates. A source catalog based on all-sky observations made by the *ROSAT* X-ray observatory is now available (Voges *et al.* 1996).

A parameter frequently used to describe X-ray emission is the distance- and stellar radius-independent logarithmic ratio of X-ray to bolometric luminosities $R_X = \log_{10} L_X/L_{BOL}$. *ROSAT* X-ray observations of G stars in open clusters found R_X values reaching a maximum "saturation" value near -3 at an age of $\sim$ 50 My (e.g., the Pleiades). Thereafter, R_X monotonically decreases with age (Randich *et al.* 1995; Prosser *et al.* 1995; Stern *et al.* 1995; Randich *et al.* 1996a; Randich *et al.* 1996b; Micela *et al.* 1996). The current quiescent X-ray luminosity of the Sun varies with the solar cycle between $2 - 6 \times 10^{27}$ erg s^{-1} (Ayres *et al.* 1996), and $R_X \approx -6.0$.

Empirical prescriptions for the evolution of the rotation period and activity of solar-mass stars derived from observations can be used to "predict" the X-ray luminosity evolution of the Sun over 4.6 Gy and estimate its X-ray luminosity at ages less than 0.8 Gy. The time-dependence of the rotation period is expressed as a power law;

$$P = P_0 \, (t/t_0)^{\alpha} \tag{3}$$

where P_0 and t_0 are the rotation period and age at X-ray "saturation" before which the X-ray luminosity, and thus solar wind and rotational braking, were independent of rotation period. The value of α which best describes the observations is debated: Skumanich (1972) first derived a value of 1/2, while $\alpha = 1/e$ has also been proposed (Walter & Barry 1991). The observed correlation between X-ray luminosity and rotation is described by

$$L_X \sim P^{-2.64} \tag{4}$$

(Güdel *et al.* 1997b, and references therein). Combining Eqns 2, 3 and 4 produces the predicted time dependence of the solar R_X value;

$$R_X = -6.0 - 2.64\alpha \log(t/4.6) + \log\left[1 + 0.4(1 - t/4.6)\right], \tag{5}$$

where t is in Gy. The X-ray emission of the Sun is at saturation ($R_X = -3$) at an age of $\sim 30 \times 10^{(\alpha-0.5)/\alpha}$ Ma.

Fig. 2 is a diagram of R_X vs. bolometric luminosity in which the trajectory of the Sun is plotted vis-a-vis Eqns. 2 and 5. At ages $t < 0.8$ Gy, the solar $R_X > -[4.86 + 2.64(\alpha - 0.5)]$, i.e.,

more than an order of magnitude greater than the present value. Hyades stars (Stern *et al.* 1995) with *ROSAT* detections or upper limits are plotted for comparison. The age of the Hyades cluster has recently been estimated at 625 ± 50 My using *Hipparcos* astrometry (Perryman *et al.* 1998). Its age, proximity (46 pc) and relative richness make this cluster well-suited for comparison with the predicted characteristics of a young Sun. The R_X values of the Hyades have been adjusted downwards by 24% to compensate for the predicted difference in luminosity between the Hyades- and solar-metallicity ZAMS at $1M_\odot$. The agreement between the predicted R_X of the Sun at 625 My and those of Hyades G dwarfs demonstrates that the Sun is not X-ray anomalous and suggest that the simple model of X-ray luminosity evolution can be used as plausible criterion for selecting young solar analogs.

The agreement between the Sun and Hyades stars is a non-trivial observation as it is not *a priori* obvious that the Sun is a "normal" rotator: The Sun at present contains only 3% of the entire angular momentum of the Solar System. Although the angular momentum in the planets is constant, and that in the Sun has decreased with time, it is likely that the Sun has always had the minority share of the angular momentum since dynamically decoupling from the protoplanetary disk. If there is some process which partitions a fixed amount of angular momentum between star and planets and this partitioning varies from system to system, stellar rotation rates and X-ray luminosities at a given age would vary considerably. Worse, stars without planetary systems would systematically rotate faster, be more X-ray luminous and appear more often in an X-ray-selected catalog. Although this scenario cannot be entirely disproved, the consistency of the predicted solar evolution in R_X with the Hyades observations does not support the hypothesis that a fixed amount of angular momentum is partitioned between planets and stars.

To argue this more quantitatively, the Sun's share of the total angular momentum is estimated at time $t = 0$ when it dynamically decoupled from the protoplanetary disk. The solar rotation period at the end of X-ray saturation was ~2 days (Eqn. 4). The evolution of the solar rotation period at earlier times is estimated by assuming that the braking torque of the solar wind is proportional to the product of the rotation rate and the wind mass loss rate (the solar radius being relatively constant), and that the latter is a function only of X-ray luminosity. Since the X-ray emission, and hence the mass loss rate, is constant at saturation, the time-dependence of the rotation period is exponential;

$$P(t) = P_0 e^{\alpha(t/t_0 - 1)}. \tag{6}$$

The rotation period extrapolated to $t = 0$ is 1.3 days. The total angular momentum in the Solar System was 1.5 times its present value and one-third of this was in the Sun. If another G star was allocated the total amount, its rotation period would be three times shorter, and it would be ~ 15 more X-ray luminous than the coeval Sun. At the age of the Hyades this hypothetical star would appear as an object with $R_X = -3.5$. (For $\alpha = 1/e$ this becomes $R_X = -4.1$). *ROSAT* observations show that such objects are very rare or nonexistent in the Hyades cluster.

The predicted value ($R_x = -4.86$) of the Sun at 0.8 Gy ($\alpha = 0.5$) is adopted as the X-ray criterion for selecting candidate young solar analogs. A residual star-to-star dispersion in

rotation rates could contaminate the sample with older but more rapidly-rotating stars. The metallicity-corrected Hyades data is used to crudely estimate the degree of this contamination. A star which has $R_X = -4.86$ (the selection limit) at 0.8 Gy will have $R_X = -4.72$ at the age of the Hyades. The equivalent metal-rich and under-luminous Hyades star would have $R_X = -4.63$. Forty percent of Hyades stars within the bolometric luminosity selection range have $R_X > -4.63$. One concludes that if the X-ray luminosity dispersion of the Hyades is representative of nearby field stars, as much as two-fifths of the X-ray selected sample will have ages somewhat greater than 0.8 Gy. Inspection of other age indicators in §5 suggests that contamination by older stars is not a serious problem.

In summary, young solar analogs are selected on the basis of (1) distances less than 25 pc; (2) lack of known companions with a projected distance of 800 AU; (3) bolometric luminosities in the range $-0.37 < \log_{10} L/L_\odot < 0.06$ and below the Hyades ZAMS for the star's effective temperature; and (4) $R_X > -4.86$.

3. Construction of the Catalog

Stars are selected from the *Hipparcos* main catalog, which contains space-based measurements of parallax, proper motion, and apparent magnitudes, and estimated spectral types for 118,218 stars (Perryman *et al.* 1997). X-ray flux measurements are from observations by the *Roentgen* X-ray satellite observatory (*ROSAT*) using the Pulse Sensitive Proportional Counter (PSPC). The PSPC was sensitive to X-rays over an energy range of about 0.2 to 2 keV and had an angular resolution of approximately 30 arc-seconds (Trümper 1983; Pfeffermann *et al.* 1986). Flux data was retrieved from the Bright Source Catalog (BSC), which contains the 18,811 brightest sources in the *ROSAT* All Sky Survey (Trümper 1993; Voges *et al.* 1996), and SRCCAT, consisting of sources detected in the entire collection of pointed observations (Voges *et al.* 1994). The *Hipparcos* catalog is complete to $V = 7.9 + 1.1 \sin |b|$ for stars bluer than $B - V = 0.8$, and to $V = 7.3 + 1.1 \sin |b|$ for redder stars, where b is the Galactic latitude. The catalog also includes fainter stars which were selected for their special astrophysical interest. The *ROSAT* BSC is 92% complete over the entire sky to a count rate of 0.1 $\sec^{-1}$, corresponding to approximately 6×10^{-13} ergs $\sec^{-1}$ cm^{-2} for the unabsorbed spectrum of a stellar corona. The X-ray flux limit can be converted to a limiting magnitude using the minimum required $R_X = -4.86$. The equivalent completeness distances for zero-age main sequence stars varies with spectral type (Fig. 3). Over the G0 to K1 range of interest the sample is essentially X-ray limited.

Most stars within 25 pc do not have accurate, spectrally-derived photospheric temperatures with which to calculate bolometric corrections and place the stars in an HR diagram. Estimates from other temperature indicators are problematic. MK spectral classifications are less sensitive to metallicity and in principle more accurate than $B - V$ colors in T_e calculations. However, different spectral classifications obtained from the literature are often inconsistent by up to three subclasses (about 120 K for a G5 star). To account for this uncertainty, two estimates of T_e are made from

the spectral type and from the $B-V$ color (these are usually, but not always, independent). Effective temperatures are estimated from spectral types using the calibration of MK standards by Gray & Corbally (1994). A second estimate of T_e from $B-V$ colors is made using fits from Flower (1996):

$$\log_{10} T_e/T_\odot = -0.012 - 0.242(B-V-0.68) + 0.136(B-V-0.68)^2 - 0.033(B-V-0.68)^3 \quad (7)$$

These estimates are compared *post facto* with available spectral-fitting values from the catalog of Cayrel de Strobel *et al.* (1997). Neither estimation technique appears superior to the other and the geometric mean is used: The standard deviation of the mean with respect to the spectral-fitting value is ~ 90 K. Bolometric luminosities are calculated via

$$\log_{10} L/L_\odot = -\left[0.1 + 0.4\,(V + B.C) + 2\log_{10}\pi\right] \quad (8)$$

where π is the stellar parallax in seconds of arc and B.C. is the bolometric correction. An empirical relation between $B.C.$ and $B-V$ from fits to the tabulations in Flower (1996) is:

$$B.C. = -0.079 + 2.363\tau - 16.085\tau^2 + 57.658\tau^3, \quad (9)$$

where $\tau = \log_{10} T_e/T_\odot$. Only stars falling within two standard error deviations of the L vs T_e selection envelope defined by the allowed luminosity range and the Hyades zero-age main sequence are retained(Fig. 1), preferentially selecting unevolved, solar-mass, solar metallicity stars and rejecting evolved stars and multiple systems. Over the effective temperature range considered, the Hyades ZAMS is well described by a fit to the data in Perryman *et al.* (1998):

$$\log_{10} L/L_\odot = 0.018 + 8.606\tau + 17.399\tau^2 + 32.489\tau^3 \quad (10)$$

X-ray source counterparts to stars are identified by calculating the angular separation between source centroids and position of the star. The maximum allowable separation to declare a match is a compromise between a larger value to identify as many real matches as possible, and a smaller value to minimize the probability of spurious matches. The latter is rigorously determined by generating an artificial *Hipparcos* catalog in which the sign of the Galactic latitude of each star is reversed, a randomizing process which preserves the large-scale distribution of stars on the sky. An adopted matching criterion of 40 arc-seconds finds nearly all possible X-ray source matches while keeping the probability of any spurious matches in the sample to 3%. X-ray luminosities are calculated from *ROSAT* PSPC count rates and *Hipparcos* parallaxes. The PSPC count rate to flux conversion factor of 6×10^{-12} ergs cm^{-2} count^{-1} used by Stern *et al.* (1995) was adopted for consistency. This conversion factor is appropriate for an unabsorbed thermal line spectrum with a temperature of ~ 2.5 MK (*ROSAT* Call for Proposals, Appendix F). While this temperature is somewhat cool compared to the corona of the most active stars, the conversion factor changes by only $\sim$20% with higher X-ray temperature and the selection process will not be substantially affected. The logarithmic ratio of X-ray to bolometric luminosities is

$$R_X = 0.4\,(V + B.C.) - 6.62 + \log_{10} c.r. \quad (11)$$

The initial list of candidates includes 61 stars, all with X-ray counterparts in the Bright Source Catalog. No new X-ray counterparts were found in the source catalog derived from the *ROSAT* pointed observations, however there are 8 stars with detections in both the BSC and pointed observation (see §4). An exhaustive query of the Stellar Information Database (SIMBAD) at the Centre de Donnees Astronomiques and a search of published high-resolution spectroscopic and speckle observations (e.g., Duncan 1981; Soderblom 1982; Soderblom 1985; McAlister *et al.* 1987; Young *et al.* 1987; McAlister *et al.* 1989; Duquennoy & Mayor 1991; Tokovinin 1992; Fekel 1997) resulted in the exclusion of 22 stars with putative or confirmed companions within 800 AU (Table 1). Although these rejected systems are not proper solar analogs, many of them could be composed of young, active stars: Binary systems with spatial separations larger than an AU are not experiencing significant tidal coupling. While stars with angular separations less than about 30 arc-seconds (800 AU at 25 pc) are not resolved in *ROSAT* PSPC imaging, the majority of the X-ray flux is probably associated with the G-type component or components, as these stars tend to have the highest absolute X-ray luminosity at a given age. Therefore visual or speckle-resolved binaries systems with a single G component are probably young.

Another star was excluded for a particular reason: HD 147513 (HR 6094) is a G5 dwarf star and a kinematic member of the 0.3 Gy-old Ursa Majoris moving group (Soderblom & Mayor 1993b). This age is consistent with its ZAMS status, chromospheric activity (Zarro & Rodgers 1983), high lithium abundance (Soderblom *et al.* 1993) and X-ray luminosity. However, it is a barium dwarf star (surface enriched in s-process elements) and has a white dwarf common proper motion companion at a projected separation of 5.7 arc-minutes (4400 AU) The system may have experienced a mass transfer event in the past when the former primary star (now the white dwarf) was on the asymptotic giant branch, leading to the observed contamination of the secondary's photosphere (Porto de Mello & Da Silva 1997). Thus while conditions around HD 147513 may be currently analogous to the young Sun, they were much less so in the past.

The 38 remaining young solar analog candiates, comprising 29 G stars and 9 early K stars, are listed in Table 2. Their locations in the Hertzsprung-Russel diagram are plotted in Fig. 4 using the more accurate temperatures from spectral fitting where available (Carney *et al.* 1994; Cayrel de Strobel *et al.* 1997; Favata *et al.* 1997) when available. Three stars with spectrally-derived temperatures now appear significantly above the Hyades ZAMS. The position of one star, HD 130948, can be explained by its high metallicity relative to the Sun ([Fe/H] = 0.20). In contrast, the other two (HD 152391 and 220182) have *low* metallicities. These anomalous objects also have the kinematics of old disk stars and are discussed further in §5.3.

Information on putative distant companions to these stars is given in Table 3. Values of R_X and the most recent (or accurate) measurements of other indicators of activity or youth are given in Table 4. Values of R'_{HK}, the logarithmic ratio of the chromospheric luminosity in the calcium H and K lines to the total photospheric emission, are taken from Soderblom (1985), Soderblom & Mayor (1993a), Henry *et al.* (1996), and Baliunas *et al.* (1996). Rotation periods are from Noyes *et al.* (1984), Henry *et al.* (1995), Donahue *et al.* (1996), Stepień & Geyer (1996)

and Güdel *et al.* (1997a). Rotational velocities ($v \sin i$) are taken from Soderblom & Mayor (1993a), Fernández-Figueroa *et al.* (1993), Fekel (1997), and de Medeiros *et al.* (1997). Lithium abundances are from Duncan (1981), Soderblom & Mayor (1993b), Soderblom *et al.* (1993), Favata *et al.* (1993), Pasquini *et al.* (1994), Favata *et al.* (1996), Zboril *et al.* (1997), and Favata *et al.* (1997).

A second catalog comprising 216 nearby solar-mass *Hipparcos* stars of *all* ages was also constructed strictly for the purpose of comparison with the young solar analog catalog (§5). This comparison sample was made by lifting the restrictions that the bolometric luminosity be less than the Hyades ZAMS and that $R_X > -4.86$. The allowed luminosity range is increased by 30% to $0.20 > \log_{10} L/L_\odot > -0.21$ (i.e., centered on the present luminosity of the Sun) to account for the luminosity evolution of solar-mass stars over the 5 Gy expected mean age of the sample (one-half the age of the Galactic disk). This adjustment keeps the mass range of the two catalogs approximately the same. Close binaries are not removed from the second catalog.

4. Nature of the X-ray Emission

Stars in the catalog of young solar analogs are selected based on X-ray emission and it is important to characterize the temporal and spectral nature of this emission and demonstrate consistency with a coronal origin. The *ROSAT* PSPC was sensitive to X-rays over the 0.1-2 keV energy range and provided limited energy resolution ($E/\Delta E \sim 3$). *ROSAT* spectral information is provided in the form of hardness ratios which parameterize the spectral slope . The hardness ratios are defined as the ratios of the total *counts* in different energy bands;

$$H_1 = \frac{h+m-s}{h+m+s}; H_2 = \frac{h-m}{h+m}, \tag{12}$$

where h (hard) is the number of counts between 0.9-2.0 keV, m (medium) is the number in 0.5-0.9 keV, and s (soft) is the number in 0.1-0.4 keV. The X-ray spectra of young stars are soft (low values of H_1 and H_2), consisting of a dominant low temperature component whose emission peaks at about 0.2 keV and a weaker, hotter component peaking at 0.8 keV (Güdel *et al.* 1997b). By contrast, weak-lined and classical T Tauri stars exhibit harder X-ray spectra with $H_1 > 0$ (Neuhäuser *et al.* 1995).

The X-ray hardness ratios of the solar analog candidates are all consistent with soft coronal emission with negligible absorption by intervening neutral hydrogen (Fig. 5). Only four of the stars fall marginally within the selection box for weak-lined or classical T Tauri defined by Neuhäuser *et al.* (1995). Thus these stars can be securely classified as young main sequence stars, not "old" T Tauri objects. The lack of T Tauri-like objects is not surprising: The T Tauri phase is expected to last only $\sim 10^7$ years (Strom *et al.* 1989) while the average age of this sample is probably much older than 10^8 years. A weak but significant correlation between H_1 and X-ray luminosity exists (Fig. 6). Application of the non-parametric Kendall-tau rank test

(Press *et al.* 1986) produces a τ value of 0.358 or a 8×10^{-5} probability that the ordering is spurious. The correlation persists if the single outlier point (HD 82443) is removed ($\tau = 0.35$ or 2×10^{-4} probability). No significant correlation is found for H_2. The trend in H_1 is opposite to that expected from changes in the response of the PSPC with X-ray temperature. Furthermore, the opposite trend would also appear if the change in spectrum were produced by intervening neutral hydrogen absorption: Fainter, more highly absorbed X-ray emission would appear harder. Rather, the phenomenon is be associated with the stellar X-ray spectra themselves and may be a manifestation of the previously observed correlation of X-ray temperature with X-ray luminosity (Gagné *et al.* 1995; Güdel *et al.* 1997b).

Eight stars in the sample are also detected in pointed observations by the *ROSAT* PSPC. A ninth, HD 26923, is excluded from this comparison as it and a companion (HD 26913) 67" away were not resolved in the lower signal-to-noise All Sky Survey. The integration times of pointed observations are typically 10-20 times longer than that of the All Sky Survey and the X-ray information is of considerably higher signal-to-noise. The R_X values reported in Table 4 incorporate this data. The pointed observations were carried out between one and three years after the All Sky Survey and a comparison between the two sets of count-rates can be used to investigate long-term coronal variability, malgré systematic errors such as a secular degradation in PSPC sensitivity. Systematic effects will tend to increase the difference between measurements at different epochs and the actual level of variability will be less than the observed level. The latter was taken to be the the fractional variance which, when added in quadrature to the measurement errors, returns a chi-squared of unity when comparing the two sets of measurements. The inferred actual variability is less than 50%, qualitatively similar to the low level of variability observed in the Hyades (Stern *et al.* 1994) and less than the variablity of the younger, more active Pleiades dwarfs, of which about one quarter exhibit quiescent X-ray variability exceeding a factor of 2 on a one-year timescale (Gagné *et al.* 1995).

5. Age-Related Properties

The eventual accurate measurement of the ages of these stars will be important in properly interpreting observations of their circumstellar environments. Meanwhile, the relative youth of this X-ray-selected catalog can be corroborated by sample statistics and other observations. The relative size of the sample is one crude estimator of its age. The ratio of the sample size to the comparison sample of all solar analogs should be proportional to the ratio of their ages, modulo different rates of star formation. However this comparison must include stars rejected because of companions for reasons of analogy (but not those with close spectroscopic companions which might be tidally coupled). It must also account for the X-ray flux limit of the young star catalog: Young K-type stars within 25 pc may have $R_X > -4.86$ but are too faint in X-rays to have been included in the *ROSAT* BSC (Fig. 3).

Complete sub-samples are culled from the 38 young analog catalog and the comparison

catalog of 216 stars. These lists include only stars with bolometric fluxes large enough such that, if $R_X > -4.86$, their X-ray fluxes would be above the completeness limits of the BSC. Stars must have apparent bolometric magnitude $V + B.C. < 6.90$ to satisfy this criterion. Excluding known spectroscopic binaries, the bright young sub-sample contains 30 stars. The bright comparison sub-sample has 173 stars. If the age of the Galactic disk is ~ 9 Gy (e.g., Leggett *et al.* 1998) and star formation has proceeded at a constant pace, the age of the sub-sample is $9 \times 30/173 \sim 1.5$ Gy. This is a very rough estimate because of the observed dispersion of X-ray luminosities among coeval stars (see §2), contamination of the sample by unknown close binaries, and changes in the star formation rate. However, the consistency between the size and expected age of the population lends credibility to the youthful nature of the selected stars. We next turn to more definitive age indicators.

5.1. X-ray Luminosities

An exact correspondence between age and X-ray luminosity would make it possible to infer an age distribution from an X-ray luminosity (or R_X) distribution. While such an ideal situation does not exist, it is nonetheless instructive to construct an X-ray-derived "age" distribution and compare it to a plausible history of star formation. Fig. 7 plots cumulative "age" distributions using two different values of the rotation evolution parameter α (see §2). The sample is complete to $R_X = -4.57$, corresponding to "ages" of 0.48 or 0.4 Gy ($\alpha = 1/2$ or $\alpha = 1/e$). The median "age" is ~0.4 Gy. If the solar neighborhood were sampling a region of constant star formation the cumulative age distribution would be linear and pass through the origin. There is a marked dearth of stars younger than ~0.3 Gy in the sample. Such a large deficit is unlikely to be from variability or deviation from the relationship between between age and X-ray luminosity. Instead, a plausible hypothesis is that the young star population is not drawn from a continuous distribution of stellar ages, but is instead dominated by discrete, coeval groups of stars, descended from individual molecular clouds and open clusters. Open clusters are gravitationally disrupted in $\sim 2 \times 10^8$ years (e.g., de la Fuente Marcos 1997), and since the Sun is not currently in such a cluster, this hypothesis would predict the observed deficit. Additional evidence for this scenario is presented in §5.3.

5.2. Rotation, Calcium Emission & Lithium

Measurements of other indicators of stellar youth or activity, i.e., rotation period, Ca H and K emission line strength, and lithium abundance are reported in the literature (Table 4). These support a young age for the sample: Values of R'_{HK}, the logarithmic ratio of chromospheric Ca H and K line flux to total photospheric flux (Noyes *et al.* 1984) are nearly all > -4.6, indicative of elevated chromospheric activity (Fig. 8). Indeed, there is substantial overlap with R'_{HK}-selected samples of field stars such as Soderblom *et al.* (1998). The strong correlation of R'_{HK} with R_X

agrees with previous results (e.g., Sterzik & Schmitt 1997) and suggests a calcium line luminosity proportional to $L_X^{0.38}$, i.e., proportional to the rotation rate. The R_X and R'_{HK} values indicate a mean age between 0.3 Gy (rotation evolution parameter $\alpha = 1/e$) and 0.5 Gy ($\alpha = 1/2$). The single star (HD 52698) with an anomolously low calcium emission compared to its X-ray flux could be explained by a change in activity level between the epochs of the spectroscopic and X-ray observations.

The available rotation period measurements also support this age range (Fig. 9). All periods are less than half that of the Sun, suggesting ages less than 0.9 Gy ($\alpha = 1/2$) or 0.5 Gy ($\alpha = 1/e$). There is a larger scatter in the points around the expected correlation, some of which could be due to the X-ray variability discussed earlier (§4). Of those stars with published lithium abundances, eighty percent have $\log N(Li) > 2$ (Fig. 10). Such high abundances are a qualitative, but not quantitative indication of stellar youth: The relationship between lithium and age is more complex than previously assumed (Michaud & Charbonneau 1991). Two stars in the sample have $\log N(Li) < 1$ and a third (HD 97334) may be lithium-poor, highlighting the ambiguity of the lithium abundance interpretation.

5.3. Kinematics

The kinematics of most of the sample are calculated using precise *Hipparcos* measurements of proper motions and parallaxes and published radial velocity measurements. The space motions with respect to the Galactic disk are relatively small because they have been subject to the gravitational perturbations of molecular clouds and other passing stars for a shorter period of time. Likewise, their velocities can contain coherent components which are the common motion shared by stars formed in the same molecular cloud. While the spatial distribution of these young solar analogs on the sky is unremarkably isotropic, searches for coherent space motions may be more fruitful. Detectable velocity coherence is expected to persist long after all evidence of spatial clustering is erased: The velocity dispersion and crossing time of open stellar clusters are typically ~ 1 km sec^{-1} and $\sim 10^7$ yrs, respectively, while the velocity dispersion of the stars in the Galactic disk are ~ 30 km sec^{-1}. Gravitationally unbound stars from a disrupted open cluster will disperse within a few crossing times, but will retain their common motion for $\sim 10^9$ yrs until the Galactic tide, other passing stars, and molecular clouds eventually destroy their coherent motions. The lifetimes of star-forming regions are of order 10^7 years, short compared to the age range considered here. Therefore the members of the descendant kinematic group are essentially a coeval group of stars whose single age can be determined more reliably than the age of individual stars. Putative moving groups have been identified on the basis of photometry and kinematics alone (e.g., Eggen 1995). The existence of a nearby 0.3 Gry-old moving group, the Ursa Major stream, has been confirmed by common high levels of chromospheric activity (Soderblom & Mayor 1993a). Evidence for a second, possibly younger nearby moving group, the Local Association, has been been found in surveys of extreme ultraviolet-selected stars and lithium rich stars (Jeffries & Jewell 1993;

Jeffries 1995).

Thirty stars in the sample have measured radial velocities in the literature: These are combined with *Hipparcos* proper motions to calculate velocities with respect to the Local Standard of Rest (LSR) using the transformation equations in Johnson & Soderblom (1987) and adopting a right-handed Galactic coordinate system with (U,V,W) in the directions of the Galactic center, rotation, and North Pole, respectively (i.e., the U direction is opposite to that of the frequently used left-handed coordinate system). The Sun's motion with respect to the LSR in right-handed coordinates is taken to be (+9.00,+11.53,+6.97) in km sec^{-1} (Binney & Tremaine 1987). The proper motions, radial velocities, and derived motions with respect to the LSR are listed in Tab. 5 and the velocities are plotted in Fig. 11(a,b). The space motions of an "old" subset of the 216-star comparison sample are also plotted in Fig. 11(c,d). These 118 stars were selected for their measured or upper limit values of $R_X < -4.86$. The contrast in velocity dispersion between the young and the old solar analog samples is readily apparent.

Three stars in the young solar analog catalog (HD numbers 73350, 152391 and 220182) are anomalous in that they are moving at speeds exceeding 50 km sec^{-1} with respect to the LSR, motions characteristic of old disk or halo stars. The high X-ray luminosities of these objects, more characteristic of young disk stars, poses a paradox. Furthermore, HD 152391 and 220182 are over-luminous with respect to the ZAMS, suggesting they are evolved stars (Fig. 4). Whether these objects are young stars imparted high peculiar motions with respect to the Galactic disk or elderly imposters masquerading as young stars is clearly relevant, and it is appropriate to to discuss these objects in some detail here. Two possible explanations for the pathological nature of these stars are (1) they have X-ray luminous companions; or (2) they experienced accretion and an increase in rotation rate by a mass transfer event (from a present or past companion), a process analogous to millisecond pulsars (Van den Heuvel 1984). A third, more speculative hypothesis is that the stars were ejected at high speed from a star-forming region by some unknown mechanism.

The incongruent high chromospheric activity and velocity (137 km sec^{-1}!) of HD 152391 (V2292 Oph) have been already noted by Soderblom (1990). The star's radial velocity is constant to within an individual measurement error of about 0.16 km sec^{-1} over a period of 9 years (Duquennoy & Mayor 1991), excluding any companion with $M > 0.1 M_{\odot}$ within $\sim$ 250 AU. This rules out any unresolved binary system and indicates that the high Ca II H and K emission and variability (Lockwood *et al.* 1997) is associated with the observed star itself. This, together with the non-significant 14 arc-second offset between the X-ray source and optical position, suggests that the X-ray emission is also associated with the star, contradicting the hypothesis of an unseen X-ray bright companion. A cursory inspection of Digitized Sky Survey images extracted from the first and second Palomar Sky Survey (epochs 1950 and 1988) failed to find any common proper motion companions brighter than $V \sim 18$ between 30 and 300 arc-seconds (500-5000 AU) of the star. This does not rule out the presence of a mass-donating companion on a wide orbit or a past companion which has escaped due to mass loss from the system.

HD 220182 is an apparently single star moving at 60 km sec^{-1} in the plane of the Galaxy. The star is a mere 15" from the X-ray source and has a high level of calcium emission ($R'_{HK} = -4.41$). Radial velocity monitoring (Tokovinin 1992, Carney *et al.* 1994) rules out the presence of a spectroscopic companion that might be the source of X-ray emission. The metallicity is approximately solar and does not suggest a mass transfer event. The final pathological case, HD 73350, is moving at 53 km sec^{-1} with respect to the LSR. It is the G0 primary of a putative triple system in which the other two components form an unresolved binary 64" away (1500 AU projected distance). The centroid of the X-ray emission is within 2" of the optical position and the X-ray luminosity suggests an age similar to the Hyades. Multiple-epoch radial velocity measurements at the $\sim$ 1 km sec^{-1} precision level exclude the possibility of additional close stellar companions (Abt *et al.* 1994). The star has a near-solar metallicity with [Fe/H] = $+0.09 \pm 0.05$ (Favata *et al.* 1997) and high lithium abundance ($\log_{10} N(Li) = 2.10$) (Favata *et al.* 1996) which contradict a mass-transfer explanation for the apparent current activity. The secondary is 2.3 visual magnitudes fainter, which, if it is physically associated with HD 73350, indicates that it a late G or early K star. The maximum orbital velocity of the wide binary is only $\sim$ 1 km sec^{-1}, small compared to its space motion. The binding energy of the system is likewise small compared to its kinetic energy in the reference frame of the LSR, making it highly improbable that it would have surved an ejection event from a star-forming molecular cloud. The nature of these three objects remain an enigma worthy of further investigation.

The LSR motions of the young stars are plotted at a smaller scale in Fig. 12(a,b), revealing the existence of two kinematic groups. Four stars (HD 26923, 41593, 72905, and 109011) are clustered around a mean velocity of (+21.1,+11.6,-3.3) with a dispersion of 2 km sec^{-1}. Their membership in the Ursa Major group has been previously established (Soderblom & Mayor 1993). Two other stars (HD 63433 and 165185) are more distant in velocity space but are possible members. The second group includes HD 166, 82443, 97334, and 206860 centered at (-4.7,-11.1,-2.1) with respect to the LSR or (-13.7,-22.6,-9.1) relative to the Sun. The dispersion in velocity is 3 km sec^{-1}. This group may correspond to the so-called Local Association whose existence was first suggested by Eggen (1983) and subsequently supported by the kinematics of active and lithium-rich stars detected in *ROSAT* Wide-Field Camera observations (Jeffries & Jewell 1993; Jeffries 1995). The mean derived here differs by 5.6 km sec^{-1} from that of Jeffries (1995). The motion in the reference frame of the Sun is 37 km sec^{-1} from the radiant at $\alpha = 276°$, $\delta = +29°$, in the constellation Hercules.

The kinematics of the eight stars lacking radial velocity information cannot be properly calculated. However, the parallaxes and proper motions are known, and using a range of plausible radial velocities it is possible to test whether these stars *could* belong to either of the two moving groups. The results of these calculations are shown in Fig. 12(c,d), where the curves correspond to the space motions of the eight stars when the radial velocities are allowed to vary from -50 to +50 km sec^{-1}. Two stars (HD 118972 and 128400) are possible members of the Ursa Major group. A third (HD 116956) could be a member of the Local Association. Thus 8, and as many as

13, stars belong to these two kinematic groups.

In summary, X-ray emission, calcium H and K emission, rotation periods, and kinematics support ages between 0.2 and 0.8 Gy for the 38 young solar analogs presented here. Four to six of these stars are members of the Ursa Major group, with a previously assigned age of 0.3 Gy. The kinematics of this X-ray-selected sample also support the existence of a second nearby kinematic group (the Local Association) but X-ray emission and other activity indicators do not suggest the existence of Pleiades-age stars in the solar neighborhood. These 38 stars are excellent analogs of the Sun, and possible the Solar System, during a period 3.8-4.4 Ga. Future observations, particularly in the thermal infrared and vacuum ultraviolet, will greatly improve our understanding of the circumstellar environment of these stars and conditions which may resemble those experienced by the early Solar System and the Earth during the origin of Life.

Acknowledgements

This work made extensive use of the the SIMBAD III database administered by the Centre des Donnees Astronomiques in Strasborg, France. The Digitized Sky Surveys were produced at the Space Telescope Science Institute using photographic data obtained at the Oschin Schmidt Telescope on Palomar Mountain and the UK Schmidt Telescope. The author acknowledges support under the NASA Origins and Astrobiology programs. He wishes to thank Joel Kastner for the many stimulating conversations from which the idea for this project arose, Michael Perryman for supplying published Hyades data in electronic form, Chris Koresko for a thorough reading of an early version of the manuscript, and Alexander Brown for a thorough and useful critiquing of the final paper.

REFERENCES

Abt, H.A., and Willmarth, D.W., 1994, ApJS, 94, 677–685.

Aumann, H. H., Beichman, C.A., Gillett, F.C., De Jong, T., Houck, J.R., Low, F.J., Neugebauer, G., Walker, R.G., and Wesselius, P.R., 1984, ApJ278, L23-L27.

Aumann, H. H., and Probst, R.G., 1991, ApJ368, 264–271.

Ayres, T. R., Simon, T., Stauffer, J. R., Sern, R. A., Pye, J. P., and Brown, A., 1996, ApJ, 473, 279–293.

Backman, D. E., and Paresce, F.,1993, in *Protostars and Planets III*, Tucson: University of Arizona Press.

Baliunas, S., Sokoloff, D., and Soon, W., 1996, ApJ, 457, L99-L102.

Beckwith, S.V.W., and Sargent, A.I., 1996, Nature, 383, 139-144.

Binney, J., and Tremaine, S., 1987, *Galactic Dynamics*, Princeton: Princeton University Press.

Boesgaard, A. M., 1989, ApJ, 336, 798–807.

Boothroyd, A.I., Sackmann, I.-J., and Fowler, W.A., 1991, ApJ, 377, 318–329.

Bowring, S.A., Williams, I. S., and Compston, W., 1989, Geology, 17, 971–975.

Canuto, V.M., Levine, J.S., Augustsson, T.R., Imhoff, C.L., and Giampapa, M.S., 1983, Nature, 305, 281.

Canuto, V.M., Levine, J.S., Augustsson, T.R., and Imhoff, C.L., 1982, Nature, 296, 816.

Carney, B.W., Lathan, D.W., Laird, J.B., and Aguilar, L.A., 1994, AJ, 107, 2240.

Carraro, G., and Chiosi, C., 1994, A&A, 287, 761–768.

Cayrel de Strobel, G., Soubiran, C., Friel, E.D., Ralite, N., and Francois, P., 1997, A&AS, 124, 299–305.

Chassefiere, E., 1997, Icarus, 129, 229-232.

Chen, H., Bally, J., O'Dell, C.R., McCaughrean, M.J., Thompson, R.L., Rieke, M., Schneider, G., Young, E.T., 1998, ApJ, 492, L173.

Cheng, K.-P., Bruhweiler, F. C., Kondo, Y., and Grady, C.A., 1992, ApJ, 396, L83–L86.

Chyba, C.F., 1987, Nature, 330, 632–635.

Chyba, C.F., Thomas, P.J., Brookshaw, L., and Sagan, C., 1990, Science, 249, 366–373.

Chyba, C.F., 1991, Icarus, 92, 217–233.

Davis, M., Hut, P., and Muller, R.A., 1984, Nature, 308, 715–717.

Donahue, R. A., Saar, S. H., and Baliunas, S. L., 1996, ApJ, 466, 384–391.

Dorren, J.D., and Guinan, E.F., 1994, ApJ, 428, 805–818.

Dorren, J.D., Güedel, M., and Guinan, E.F., 1995, ApJ, 448, 431–436

Drake, J.J., Stern, R.A., Stringfellow, G.S., Mathioudakis, M., Laming, J. M., and Lambert, D. L., 1996, ApJ, 469, 828–833.

Duncan, D. K., 1981, ApJ, 248, 651–669

Duquennoy, A., and Mayor, M., 1991, A&A, 248, 485–524.

Eggen, O.J., 1983, AJ, 88, 642.

Eggen, O.J., 1995, AJ, 110, 1749–1761.

Fajardo-Acosta, S.B., Stencel, R.E., and Backman, D.E., 1997, ApJ, 487, L151.

Favata, F., Barbera, M., Micela, G., and Sciortino, S., 1993, A&A, 277, 428–438.

Favata, F., Micela, G., and Sciorino, G., 1996, A&A, 311, 951–960.

Favata, F., Micela, G., and Sciortino, S., 1997, A&A, 322, 131-138.

Fegley, B., Jr., Prinn, R.G., Hartman, H., and Watkins, G.H., 1986, Nature, 319, 305.

Feigelson, E.D., 1982, Icarus, 51, 155–163.

Fekel, F. C., 1997, PASP, 109, 514–523.

Fernandez, J.A., and Ip, W.-H., 1983, Icarus, 54, 377–387.

Fernández-Figueroa, M.J., Barrado, D., De Castro, E., and Cornide, M., 1993, A&A, 274, 373–380.

Fleming, T.A., Schmitt, J.H.M.M., and Giampapa, M.S., 1995, ApJ, 450, 401–410.

Flower, P.J., 1996, ApJ, 469, 355–365.

de la Fuente Marcos, 1997, A&A, 322, 764–777.

Gagné, M., and Caillault, J.-P., and Stauffer, J.R., 1995, ApJ, 450, 217–232.

Gahm, G. F., Zinnecker, H., Pallavicini, R., and Pasquini, L., 1994, A&A, 282, 123–126.

Giampapa, M.S., Rosner, R., Kashyap, V., Fleming, T.A., Schmitt, J.H.M.M., and J.A. Bookbinder, 1996, ApJ, 463, 707–725.

Gonzalez, G., 1997, MNRAS, 285, 403–412.

Gough, D.O., 1981, Solar Phys., 74, 21–34.

Graedel, T.E., Sackmann, I.-J., and Boothroyd, A.I., Geophys. Res. Lett., 18, 1881–1884.

Gray, R.O., and Corbally, C.J., 1994, 107, 742–746.

Güdel, M., Guinan, E.F., Mewe, R., Kaastra, J.S., and Skinner, S.L., 1997a, ApJ, 479, 416–426.

Güdel, M., Guinan, E. F., and Skinner, S. L, 1997b, ApJ, 483, 947–960.

Hale, A., 1994, AJ, 107, 306–332.

Heisler, J., and Tremaine, S., 1986, Icarus, 65, 13–26.

Hempelmann, A., Schmitt, J.H.M.M., Schultz, M., Rüdiger, G., and Stepieǹ, K., 1995, A&A, 294, 515–524.

Henry, G. W., Fekel, F. C., Hall, D. S., 1995, AJ, 110, 2926–2967

Henry, T. J., Soderblom, D. R., Donahue, R. A., and Baliunas, S. L., 1996, AJ, 111, 439–465.

Holman, M., Touma, J., and Tremaine, S., 1997, Nature, 386, 254-256.

Innanen, K.A., Zheng, J.Q., Mikkola, S., and Valtonen, M.J., 1997, AJ, 113, 1915–1919.

Ip, W.-H., and Fernandez, J.A., 1988, Icarus, 74, 47–61.

Jakosky, B.M., Pepin, R.O., Johnson, R.E., and Fox, J.L., 1994, Icarus, 111, 271–288.

Jeffries, R.D., and Jewell, S.J., 1993, 264, 106–120.

Jeffries, R.D., 1995, MNRAS, 273, 559.

Jewitt, D. C., 1994, AJ, 108, 661–665.

Johnson, D.R.H., and Soderblom, D.R., 1987, AJ, 93, 864.

Kalas, P., and Jewitt, D., 1996, AJ, 111, 1347.

Kasting, J.F., 1991, in *The Sun in Time*, C.P. Sonett, M.S. Giampapa, and M.S. Matthews, eds., Tucson: University of Arizona Press.

Kasting, J.F., 1993, Science, 259, 920–1061.

Landi, E., Landini, M., and Del Zanna, G., 1997, A&A, 324, 1027–1035.

Leggett, S.K., Ruiz, M.T., and Bergeron, P., 1998, ApJ, 497, 294.

Lindroos, K.P., 1986, A&A, 156, 223–233.

Lockwood, G. W., Skiff, B. A., and Radick, R. R., 1997, ApJ, 485, 789–811.

Maas, R., Kinny, P.D., Williams, I.S., Froude, D. O, and Compston, W., 1992, Geochimica et Cosmochimica Acta, 56, 1281–1300.

Maggio, A., Vaiana, G. S., Haisch, B. M., Stern, R. A., Bookbinder, J., Harnden, F. R., Jr., and Rosner, R., 1990, ApJ, 348, 253–278.

Maher, K.A., and Stevenson, D. J., 1988, Nature, 331, 612–614.

Mannings, V., and Sargent, A.I., 1997, ApJ, 490, 792.

Mathioudakis, M., Fruscione, A., Drake, J.J., McDonald, K., Bowyer, S., and Malina, R.F., 1995, A&A, 300, 775–782.

McAlister, H. A., Hartkopf, W. I., Sowell, J. R., Dombrowski, E. G., and Franz, O. G., 1989, AJ, 97, 510–531.

McAlister, H. A., Hartkopf, W. I., Hutter, D. J., Shara, M. M., and Franz, O. G., 1987, AJ, 93, 183–194.

McCaughrean, M., and O'Dell, C.R., 1996, AJ, 111, 1977.

de Medeiros, J.R., do Nascimento, J.D., Jr., and Mayor, M., A&A, 317, 701–706.

Mennesson, B., and Mariotti, J.-M., 1997, *Icarus*, 128, 202–212.

Messina, S., and Guinan, E.F, 1996, Information Bulletin on Variable Stars, 4286, 1.

Micela G., Sciortino S., Kashyap V., Harnden F.R., and Rosner, R., 1996, A&AS, 102, 75.

Michaud, G., and Charbonneau, P., 1991, Space Sci. Rev., 57, 1.

Moneti, A., Zinnecker, H., Kunkel, M., and Preibish, T., 1997, in Star Formation with the Infrared Space Observatory, J. Yun and R. Liseau, eds., ASP Conference Series, 132, 281.

Neuhäuser, R., Sterzik, M. F., Schmitt, J.H.M.M., Wichmann, R., and J. Krautter, 1995, A&A, 295, L5-L8.

Noyes R.W., Hartmann, L.W., Baliunas, S.L., Duncan, D.K., and Vaughan, A.H., 1984, ApJ, 279, 763–777.

Pasquini, L., Liu, Q., and Pallavicini, R., 1994, A&A, 287, 191–205.

Perez-de-Tejada, H., 1992, J. Geophys. Res., 97, 3159–3167.

Perryman, M.A.C., Lindegren, L., Kovalevsky, J., Hog, E., Bastian, U., Bernacca, P.L., Créze, M., Donati, F., Grenon, M., Grewing, M., van Leeuwen, F., van der Marel, H., Mignard, F., Murray, C.A., Le Poole, R.S., Schrijver, H., Turon, C., Arenou, F., Froeschlé, M., and Petersen, C.S., 1997, A&A, 323, L49–L52.

Perryman, M.A.C., Brown, A.G.A., Lebreton, Y., Gomez, A., Turon, C., Cayrel de Strobel, G., Mermilliod, J.C., Robichon, N., Kovalevsky, J., Crifo, F., A&A, 1998, 331, 81–120.

Pfeffermann, E., Briel, U. G., Hippmann, H., et al., 1986, Proc. SPIE, 73, 519.

Porto de Mello, G.F., and Da Sila, L., ApJ, 476, L89.

Press, W. H., Flannery, B. P., Teukolsky, S. A. and W. T. Vetterling, *Numerical Recipes*, Cambridge: Cambridge University Press (1986).

Prosser, C.F., Stauffer, J.R., Caillault, J.-P., Balachandran, S., Stern, R.A., and Randich, S., 1995, AJ, 110, 1229–1247.

Randich, S., Schmitt, J.H.M.M., Prosser, C.F., and Stauffer, J.R., 1995, A&A, 300, 134–157.

Randich, S., Schmitt, J.H.M.M., Prosser, C.F., and Stauffer, J.R., 1996a, A&A, 305, 785–805.

Randich, S., Schmitt, J.H.M.M., and Prosser, C., 1996b, A&A, 313, 815–827.

Ray, T., Sargent, A.I., Beckwith, S.W., Koresko, C., and Kelly, P., 1995, ApJ, 440, L89–L92.

Sargent, A.I., and Beckwith, S.V.W., Astroph. Space Sci., 212, 181–189.

Schmitt, J. H. M. M., Golub, L., Harnden, F. R., Jr., Maxson, C. W., Rosner, R., and Vaiana, G.S., 1985, ApJ, 290, 307–320.

Schmitt, J.H.M.M., Fleming, T.A., and Giampapa, M.S., 1995, ApJ, 450, 392–400.

Simon, T., Drake, S. A., and Kim, P.D., 1995, PASP, 107, 1034–1041.

Simon, T., and Landsman, W.B., 1997, ApJ, 483, 435–438.

Skumanich, A., 1972, ApJ, 171, 565–567.

Smith, B. A., and Terrile, R.J., 1984, Science, 226, 1421–1424.

Soderblom, D. R., 1982, ApJ, 1982, 263, 239–251.

Soderblom, D. R., 1985, AJ, 90, 2103–2115.

Soderblom, D. R., and Mayor, M., 1993a, AJ, 105, 226–249.

Soderblom, D. R., and Mayor, M., 1993b, ApJ, 402, L5–8.

Soderblom, D. R., Pilachowski, C. A., Fedele, S. B., and Jones, B. F., AJ, 1993, 105, 2299–2307.

Soderblom, D. R., King, J. R., Hanson, R.B., Jones, B. F., Fischer, D., Stauffer, J. R., and Pinsonneault, M. H., 1998, astro-ph/9801281 preprint.

Sonett, C.P., Giampapa, M.S., Matthews,M.S., eds., *The Sun in Time*, Tucson: U. of Arizona Press (1991).

Stauffer, J.R., and Soderblom, D.R., 1991, *The Sun in Time*, C.P. Sonett, M.S. Giampapa, and M.S. Matthews, eds., Tucson: University of Arizona Press.

Stevenson, D.J., and Lunine, J.I., 1988, Icarus, 75, 146–155.

Stencel, R. E., and Backman, D.E., 1991, ApJS, 75, 905–924.

Stepień, K., and Geyer, E., 1996, A&AS, 117, 83–91.

Stern, R.A., Schmitt, J.H.M.M., Pye, J.P., Hodgkin, S.T., Stauffer, J.R., and Simon, T., 1994, ApJ, 427, 808–821.

Stern, R.A., Schmitt, J.H.M.M., and Kahabka, P.T., 1995, ApJ, 448, 683–704.

Sterzik, M.F., and Schmitt, J.H.M.M., 1997, AJ, 114, 1673–1678.

Strassmeier, K.G., and Rice, J.B., 1998, A&A, 330, 685–695.

Strom, K. M., Strom, S. E., Edwards, S., Cabrit, S., and M. F. Skrutskie, 1989, AJ, 97, 1451–1470.

Tokovinin, A.A., 1992, A&A, 256, 121–132.

Trümper, J., 1983, Adv. Space Res., 2, 241.

Trümper, J., 1993, Science, 260, 1769.

Tsikoudi, V., 1989, AJ, 98, 290–296.

Tsikoudi, V., 1990, AJ, 100, 1618–1620.

Van den Heuvel, E.P.J., 1984, J. Astrophys. Astron., 5, 209–233.

Voges, W., Gruber R., Haberl F., Kürster M., Pietsch W., and Zimmermann U., 1994, ROSAT NEWS No. 32.

Voges, W., Aschenbach, B., Boller, T., Brüninger, H, Briel, U., Burkert, W., Dennerl, K., Englhauser, J., Gruber, R., Haberl, F., Hartner, G., Hasinger, G., Kürster, M., Pfeffermann, E., Pietsch, W., Predehl, P., Rosso, C., Schmitt, J. H. M. M., Trümper, J., and H.-U. Zimmermann, 1996, submitted to A&A.

Waelkens, C., Waters, L.B.F.M.; de Graauw, M.S., Huygen, E., Malfait, K., Plets, H., Vandenbussche, B., Beintema, D.A., Boxhoorn, D.R., Habing, H.J., Heras, A.M., Kester, D.J.M., Lahuis, F., Morris, P.W., Roelfsema, P.R., Salama, A., Siebenmorgen, R., Trams, N.R., Van derBliek, N.R., Valentijn, E.A., and Wesselius, P.R., A&A, 315, L245-L248.

Walker, H. J., and Wolstencroft, R.D., 1988, PASP, 100, 1509–1521.

Walter, F. M., and Barry, D.C., 1991, in *The Sun in Time*, C.P. Sonett, M.S. Giampapa, and M.S. Matthews, eds., Tucson: University of Arizona Press.

Weinberg, M.D., Shapiro, S.L., and Wasserman, I., 1987, ApJ, 312, 367–389.

Weissman, P.R., 1989, in *Origin and Evolution of Planetary and Satellite Atmospheres*, S.K. Atreya, J.B. Pollack and M.S. Matthews, eds., Tucson: University of Arizona Press.

Wetherill, G. W., 1994, Astrophys. & Space Sci., 212, 23–32.

Whitmire, D.P., Doyle, L.R., Reynolds, R.T., and Metese, J.J., 1995, JGR, 100, 5457–5464.

Wolff, S. C., and Simon, T., 1997, PASP, 109, 759–775.

Young, A., Mielbrecht, R.A., Abt, H.A., 1987, ApJ, 317, 787–795.

Zahnle, K.J., and Walker, J.C.G., 1982, Rev. Geophysics and Space Physics, 20, 280–292.

Zarro, D.M., and Rodgers, A.W., 1983, ApJS, 53, 81.

Zboril, M., Byrne, P.B., and Rolleston, W.R.J.R., 1997, MNRAS, 284, 685–691.

Fig. 1.— Schematic of the selection envelope for young solar analogs in the Hertzsprung-Russel diagram. The positions of the Sun at its arrival on the main sequence (zero age) and the present are marked.

Fig. 2.— The predicted trajectory of the Sun from 32 Myr to the present in a plot of specific X-ray luminosity R_X versus bolometric luminosity. Ages of 70 and 625 Myr correspond to those of the Pleiades and Hyades clusters. Hyades detections (filled points) and upper limits (open points) from Stern *et al.* (1995) are plotted for comparison. The selection box for young solar analogs is also shown: The lower boundary of the box corresponds to the predicted solar value of R_x at an age of 0.8 Gyr.

Fig. 3.— The completeness limits of the *Hipparcos* and *ROSAT* catalogs for stars on the solar-metallicity zero-age main sequence. The dashed box marks the 25 pc distance limit and the approximate range of allowed spectral types.

Fig. 4.— Hertzsprung-Russel diagram of the 38 young solar analogs. Filled points are stars with effective temperatures determined from spectral fitting. Open points are stars with effective temperatures estimated from spectral type and $B-V$ color. The dashed line is the solar-metallicity ZAMS; the solid line is the Hyades ZAMS.

Fig. 5.— X-ray hardness ration (defined in the text) for the 38 candidate young solar analogs. The dashed box is the envelope for weak-lined T Tauri stars defined by Neuhäuser *et al.* (1995).

Fig. 6.— *ROSAT* X-ray luminosity R_X vs. hardness-ratio H_1 demonstrating a significant positive correlation.

Fig. 7.— Age distribution of the sample assuming two values of the rotation evolution parameter α. The samples are complete to ages 0.48 Gyr ($\alpha = 1/2$) or 0.4 Gyr ($\alpha = 1/e$) (dashed line).

Fig. 8.— Calcium H and K emission vs. X-ray emission. The median error cross is plotted in the upper left. The dashed line marks the X-ray selection cut-off for the sample. The Sun is plotted in the lower left and the solid line is the expected evolution if calcium emission is proportional to rotation rate and thus $L_X^{0.38}$. Ages on the evolutionary track assume a rotation evolution parameter $\alpha = 1/2$.

Fig. 9.— Rotation rate vs. X-ray emission. The median error in R_X is shown in the upper left: Formal errors for rotation periods are negligible by comparison. The dashed line marks the X-ray selection cut-off for the sample. The Sun is plotted in the lower left and the solid line is the expected evolution if $L_X \sim P^{-2.64}$. Ages on the evolutionary track assume a rotation evolution parameter $\alpha = 1/2$.

Fig. 10.— Lithium abundance vs. X-ray emission. The median error in R_X is plotted in the upper left hand corner: Literature values of N(Li) almost never included formal uncertainties.

Fig. 11.— (a,b) (top) Kinematics of 30 young solar analogs with respect to the Local Standard of Rest (see text for calculation details). The Sun is plotted as the circled point..(c,d) (bottom) Kinematics of "old" solar analogs for comparison, demonstrating the larger dispersion in velocities.

Fig. 12.— (a,b) (top) Kinematics of the 30 young solar analogs at a smaller scale, showing the clustering in velocity space. The motion of the Sun is plotted as a circled point and the location of the Ursa Major and Hercules kinematic groups disccussed in the text are labeled. (c,d)(bttom) Kinematics of the remaining 8 young solar analogs as a function of unknown radial velocity ranging from -50 to +50 km sec^{-1}. The location of the two Ursa Major group and Local Association are marked and the trajectories of possible group members are heavy lines.

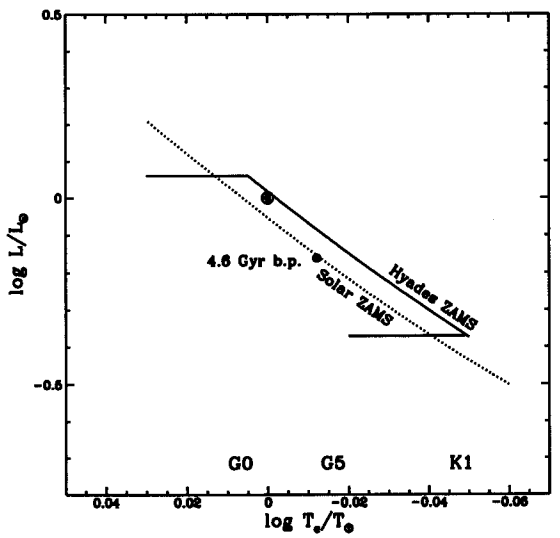

Fig. 1.— Schematic of the selection envelope for young solar analogs in the Hertzsprung-Russel diagram. The positions of the Sun at its arrival on the main sequence (zero age) and the present are marked.

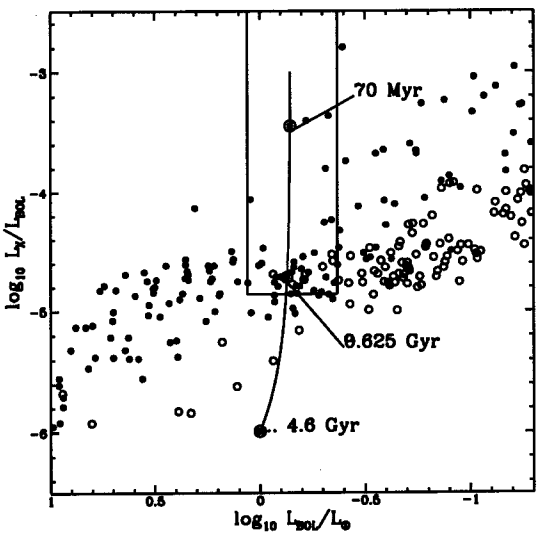

Fig. 2.— The predicted trajectory of the Sun from 32 Myr to the present in a plot of specific X-ray luminosity R_X versus bolometric luminosity. Ages of 70 and 625 Myr correspond to those of the Pleiades and Hyades clusters. Hyades detections (filled points) and upper limits (open points) from Stern *et al.* (1995) are plotted for comparison. The selection box for young solar analogs is also shown: The lower boundary of the box corresponds to the predicted solar value of R_x at an age of 0.8 Gyr.

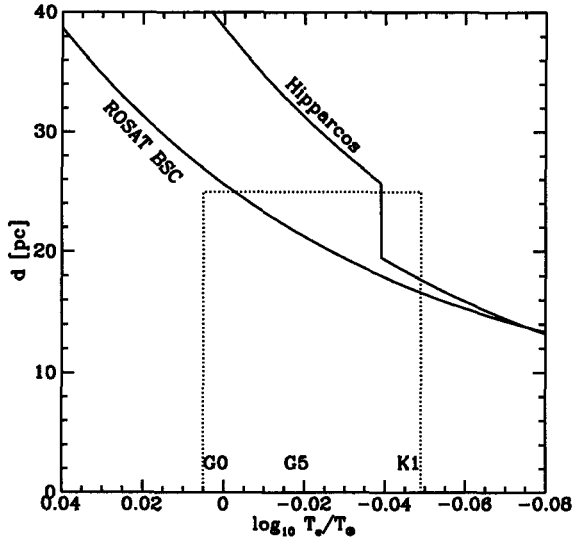

Fig. 3.— The completeness limits of the *Hipparcos* and *ROSAT* catalogs for stars on the solar-metallicity zero-age main sequence. The dashed box marks the 25 pc distance limit and the approximate range of allowed spectral types.

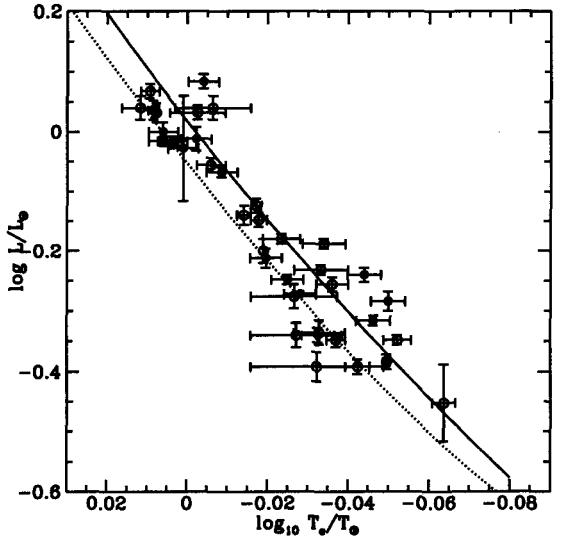

Fig. 4.— Hertzsprung-Russel diagram of the 38 young solar analogs. Filled points are stars with effective temperatures determined from spectral fitting. Open points are stars with effective temperatures estimated from spectral type and $B-V$ color. The dashed line is the solar-metallicity ZAMS; the solid line is the Hyades ZAMS.

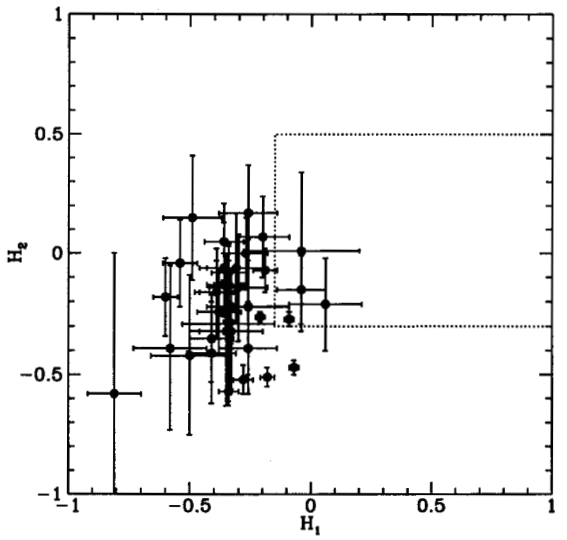

Fig. 5.— X-ray hardness ration (defined in the text) for the 38 candidate young solar analogs. The dashed box is the envelope for weak-lined T Tauri stars defined by Neuhäuser *et al.* (1995).

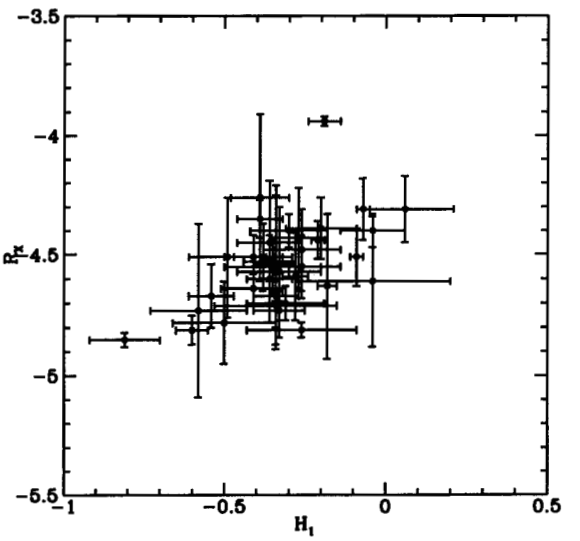

Fig. 6.— *ROSAT* X-ray luminosity R_X vs. hardness-ratio H_1 demonstrating a significant positive correlation.

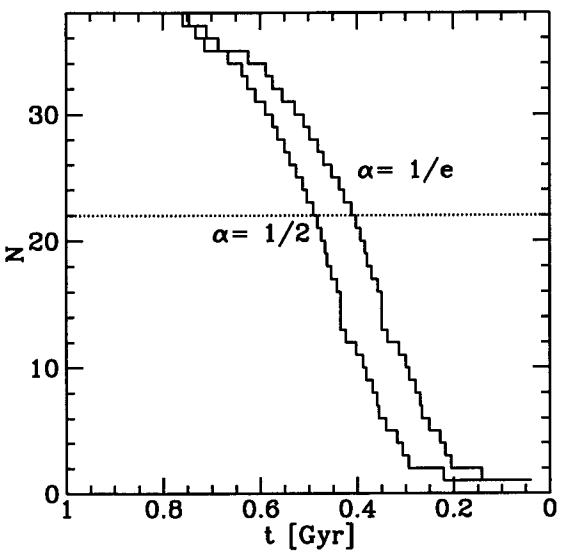

Fig. 7.— Age distribution of the sample assuming two values of the rotation evolution parameter α. The samples are complete to ages 0.48 Gyr ($\alpha = 1/2$) or 0.4 Gyr ($\alpha = 1/e$) (dashed line).

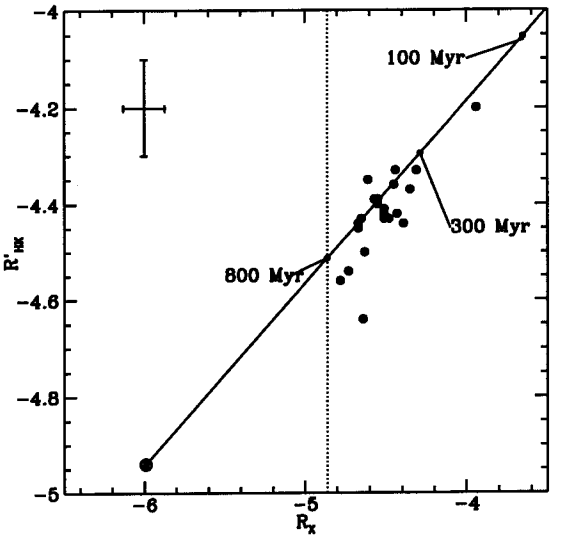

Fig. 8.— Calcium H and K emission vs. X-ray emission. The median error cross is plotted in the upper left. The dashed line marks the X-ray selection cut-off for the sample. The Sun is plotted in the lower left and the solid line is the expected evolution if calcium emission is proportional to rotation rate and thus $L_X^{0.38}$. Ages on the evolutionary track assume a rotation evolution parameter $\alpha = 1/2$.

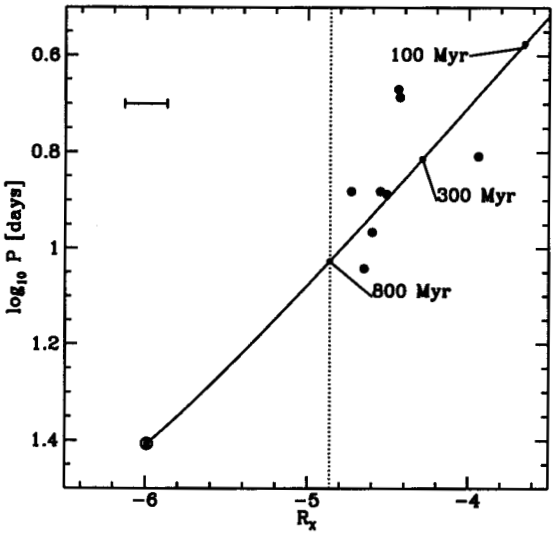

Fig. 9.— Rotation rate vs. X-ray emission. The median error in R_X is shown in the upper left: Formal errors for rotation periods are negligible by comparison. The dashed line marks the X-ray selection cut-off for the sample. The Sun is plotted in the lower left and the solid line is the expected evolution if $L_X \sim P^{-2.64}$. Ages on the evolutionary track assume a rotation evolution parameter $\alpha = 1/2$.

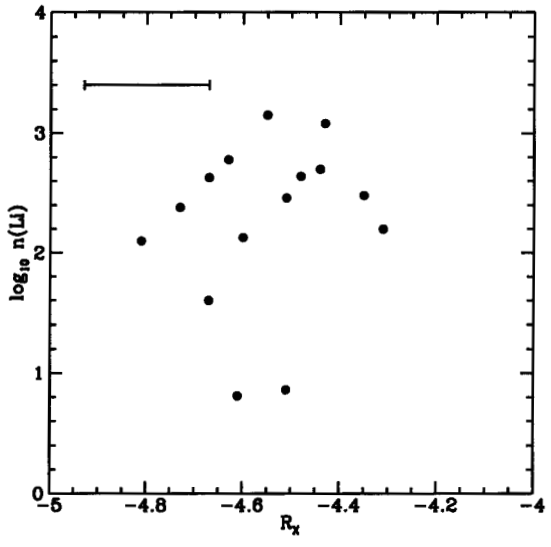

Fig. 10.— Lithium abundance vs. X-ray emission. The median error in R_X is plotted in the upper left hand corner: Literature values of N(Li) almost never included formal uncertainties.

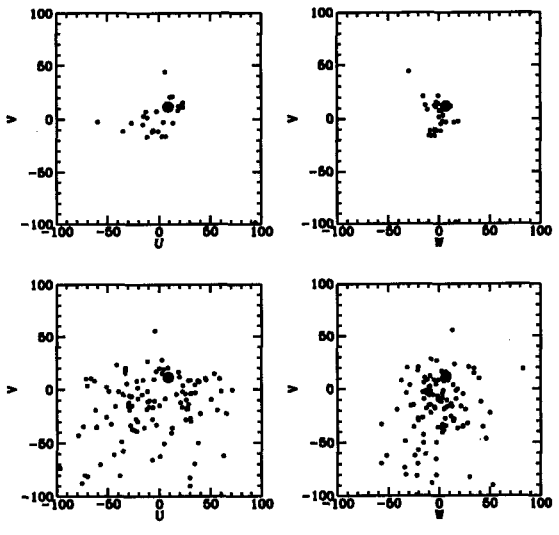

Fig. 11.— (a,b) (top) Kinematics of 30 young solar analogs with respect to the Local Standard of Rest (see text for calculation details). The Sun is plotted as the circled point..(c,d) (bottom) Kinematics of "old" solar analogs for comparison, demonstrating the larger dispersion in velocities.

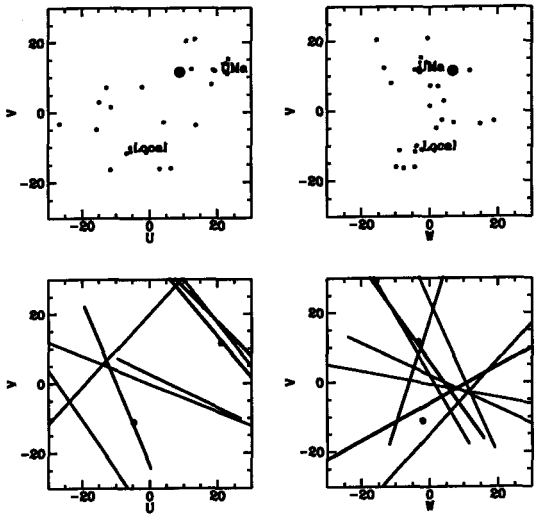

Fig. 12.— (a,b) (top) Kinematics of the 30 young solar analogs at a smaller scale, showing the clustering in velocity space. The motion of the Sun is plotted as a circled point and the location of the Ursa Major and Hercules kinematic groups discussed in the text are labeled. (c,d)(bttom) Kinematics of the remaining 8 young solar analogs as a function of unknown radial velocity ranging from -50 to +50 km sec^{-1}. The location of the two Ursa Major group and Local Association are marked and the trajectories of possible group members are heavy lines.

Table 1: Stars Rejected for Multiplicity

HD	Comment
4391	CD-48 176B $\Delta V = 7.7$ star at 16" (240 A.U.)
17382	long period spectroscopic binary
21175	δ V = 4.4 companion 2.1" (36 A.U.) away
23484	spectroscopic binary
25680	spectroscopic binary
25893	binary with $a = 86$ A.U. and $e = 0.25$
26913	spectroscopic binary
37572	SAO 217429 with $\Delta V = 1.89$ at 18" (440 A.U.)
39587	spectroscopic binary
42807	probable spectroscopic binary
45088	dM companion 15" (220 A.U.) away
45270	dM companion 16" (380 A.U.) away
54371	spectroscopic binary
72946	multiple system with two companions within 250 A.U.
96064	dM3 companion 15" (270 A.U.) away
131156	G+K binary: $a = 31$ A.U., $e = 0.51$
137778	probable spectroscopic binary
139813	common proper-motion binary with HD 139777 32" (700 A.U.) away
147513	Barium star with WD companion; possible mass transfer
149806	close dM companion distance unknown
181321	close binary of unknown separation
200968	dK binary with 4.7" (83 A.U.) separation
211472	close binary

Table 2: Young Solar Analogs

HD			d pc	V	$U-B$	$B-V$	$L/L_\odot$	T_e kelvins	[Fe/H]
166		K0	13.7	6.07	0.30	0.75	0.65	—	—
1237		G6	17.6	6.59	—	0.75	0.66	—	—
1835	BE Cet	G3	20.4	6.39	0.09	0.66	1.00	5860	-0.09
7590		G0	23.6	6.59	—	0.59	1.03	—	—
10008		G5	23.6	7.66	—	0.80	0.46	—	—
10780		K0	10.0	5.63	0.40	0.80	0.53	5419	+0.36
11131	χ Cet B	G1	23.0	6.72	0.12	0.65	0.83	5793	-0.06
20630	κ Cet	G5	9.2	4.84	0.20	0.68	0.86	5667	-0.01
26923	V774 Tau	G0	21.2	6.32	0.08	0.57	1.10	—	—
30495	58 Eri	G1	13.3	5.49	0.13	0.63	0.96	5829	-0.13
36435		G5	19.6	6.99	0.27	0.75	0.56	5458	-0.02
37394		K1	12.2	6.21	0.50	0.84	0.48	5196	-0.20
41593		K0	15.5	6.76	0.42	0.81	0.46	5362	+0.08
43162		G5	16.7	6.37	—	0.71	0.71	—	—
52698		K1	14.6	6.71	0.59	0.88	0.45	—	—
59967		G3	21.8	6.66	—	0.64	0.88	—	—
63433		G5	21.8	6.90	—	0.68	0.72	—	—
72760		G5	21.8	7.32	—	0.79	0.53	—	—
72905	π^1 UMa	G2	14.3	5.63	0.07	0.62	0.96	5860	-0.08
73350		G0	23.6	6.58	0.17	0.65	0.97	5750	+0.09
82443	DX Leo	K0	17.7	7.05	0.33	0.78	0.45	—	—
97334		G0	21.7	6.41	0.12	0.60	1.08	—	—
109011		K2	23.7	8.08	0.62	0.94	0.35	—	—
113449		G5	22.1	7.69	—	0.85	0.41	—	—
116956		G9	21.9	7.29	—	0.80	0.55	—	—
118972		K1	15.6	6.92	0.39	0.86	0.41	—	—
128400		G5	20.3	6.73	—	0.71	0.75	—	—
128987		G6	23.6	7.24	—	0.71	0.63	—	—
130948		G2	17.9	5.86	0.01	0.58	1.21	5727	+0.20
135599		K0	15.6	6.92	—	0.83	0.41	—	—
141272		G8	21.3	7.44	—	0.80	0.46	—	—
152391	V2292 Oph	G8	16.9	6.65	0.32	0.75	0.58	5233	-0.21
165185		G3	17.4	5.94	0.07	0.62	1.08	—	—
180161		G8	20.0	7.05	0.42	0.80	0.59	—	—
203244		G5	20.5	6.98	—	0.72	0.61	5525	-0.21
206860	HN Peg	G0	18.4	5.96	0.04	0.59	1.17	—	—
217813	MT Peg	G5	24.3	6.65	0.10	0.62	1.10	—	—
220182		K1	21.9	6.58	0.41	0.80	0.52	5153	-0.09

Table 3: Young Solar Analogs with Distant Companions

HD	ρ [arc-sec]	ρ [A.U.]	Companion	Spectral Type	Notes
166	61	830	BD+28 4704 B	$\Delta B = 2.8$	
166	161	2210	IDS 00014+2829 C	$\Delta B = 3.9$	
166	164	2250	IDS 00014+2829 D		
1835	164	3860	BD-13 60 B	$\Delta V = 6.1$	
11131	183	4200	χ Cet A	F3III	common μ and v_R
26923	68	1430	HD 26923	G5V	common μ
37394	98	1200	HD 233153	M0.5	common μ
73350	64	1500	BD-06 2664BC		
82443	53	940	GJ 354.1B	$V = 14.7$ M5.5	
97334	87	1890	BD+36 2162C	$V = 12.3$	

Table 4: Activity Indicators of Young Solar Analogs

HD	R'_{HK}	EUVE ct sec^{-1}	R_X	P_{ROT} days	v sin i km sec^{-1}	log N(Li)
166	-4.33	0.024	-4.36	—	—	2.2
1237	-4.44	—	-4.39	—	—	—
1835	-4.43	—	-4.60	7.7	—	2.46
7590	—	—	-4.70	—	—	—
10008	—	—	-4.40	—	—	—
10780	—	—	-4.81	—	0.6	—
11131	-4.37	—	-4.35	—	3.4	2.48
20630	—	0.032	-4.60	9.24	3.9	2.13
26923	-4.50	—	-4.39	—	4.3	2.78
30495	-4.54	—	-4.73	7.6	—	2.39
36435	-4.44	—	-4.67	—	—	1.60
37394	-4.43	—	-4.57	11	—	—
41593	-4.42	—	-4.51	—	4.0	0.86
43162	—	—	-4.26	—	—	—
52698	-4.64	—	-4.64	—	—	—
59967	-4.36	—	-4.45	—	—	—
63433	—	—	-4.51	—	—	—
72760	—	—	-4.71	—	—	—
72905	-4.33	—	-4.47	4.68	9.5	2.70
73350	—	—	-4.32	—	—	2.10
82443	-4.20	0.037	-3.94	6.43[a]	6.2	—
97334	-4.40	0.021	-4.55	7.6	—	<1.50[b]
109011	-4.35	—	-4.61	—	5.2	0.81
113449	—	—	-4.31	—	5.3	—
116956	—	—	-4.40	—	—	—
118972	-4.39	—	-4.57	—	—	—
128400	-4.56	—	-4.78	—	—	—
128987	—	—	-4.73	—	—	—
130948	-4.45	0.024	-4.67	—	—	2.63
135559	—	—	-4.37	—	—	—
141272	—	—	-4.37	—	—	—
152391	-4.39	—	-4.39	11.43	—	—
165185	-4.43	—	-4.48	—	7.5	2.64
180161	—	—	-4.61	—	—	—
203244	-4.39	—	-4.55	—	—	1.65
206860	-4.42	0.018	-4.43	4.86	11	3.08
217813	—	—	-4.53	—	—	—
220182	-4.41	—	-4.51	—	—	—

Note. — [a]Messina & Guinan (1996) report $P_{ROT} = 5.40$ days. [b]Duncan (1981) found $\log N(Li) = 2.38$;

Table 5: Space Motions of Young Solar Analogs

HD	π	μ_α	μ_δ	ρ	U	V	W
	mas	mas yr^{-1}			km sec^{-1}		
166	72.98	379.9	-178.3	-8.2	-5.5	-11.2	-2.2
1835	49.05	394.3	60.5	-2.6	-26.7	-3.3	7.1
10780	100.24	582.0	-246.8	2.8	-15.7	-4.9	2.0
11131	43.47	-122.6	-100.4	-4.2	13.7	-3.7	14.8
20630	109.18	268.9	93.5	18.9	-12.7	7.1	2.6
26923	47.20	-109.4	-108.3	-7.1	23.0	11.0	-2.8
30495	75.10	130.4	169.2	21.7	-14.9	2.9	4.3
36435	51.10	-148.9	-92.8	12.9	18.4	8.0	-11.2
37394	81.69	2.7	-523.6	-11.0	6.4	-16.0	-9.7
41593	64.71	-122.3	-103.3	-9.8	19.4	11.8	-4.2
43162	59.90	-47.1	110.9	21.7	-11.4	1.5	0.1
52698	68.42	206.6	40.9	12.6	4.2	-2.8	18.9
59967	45.93	-87.8	53.8	8.6	-2.1	7.3	0.3
63433	45.84	-9.3	-11.8	-15.7	22.5	14.0	-0.8
72905	70.07	-27.7	87.9	-12.7	18.9	12.1	-3.1
73350	42.32	-298.4	43.3	-35.3	6.2	44.1	-29.3
82443	56.35	-147.5	-246.3	8.2	-0.8	-11.4	1.6
97334	46.04	-248.6	-151.3	-3.7	-6.7	-11.7	-4.1
109011	42.13	99.7	-13.2	-13.1	23.1	11.3	-3.1
113449	45.20	-189.8	-219.6	0.0	3.1	-16.1	-4.3
130948	55.73	144.7	32.4	-2.7	13.4	21.0	-0.6
135559	64.19	178.0	-136.5	-12.0	12.5	12.4	-13.2
141272	46.84	-176.2	-166.7	-28.4	-11.5	-16.4	-7.5
152391	59.04	-711.8	-1483.7	44.9	94.0	-98.8	16.4
165185	57.58	105.4	8.0	15.2	23.3	15.3	-2.4
180161	50.00	217.8	408.3	-27.9	-35.0	-11.3	-8.7
203244	48.86	140.9	169.4	11.5	10.9	20.5	-15.5
206860	54.37	231.1	-113.4	-17.0	-5.6	-10.1	-3.8
217813	41.19	-117.7	-28.1	-3.2	22.4	11.6	11.9
220182	45.63	636.2	219.2	7.0	-59.8	-2.6	3.7